Available online at www.sciencedirect.com

ScienceDirect

Mendeleev Commun., 2022, **32**, 495–497

Mendeleev Communications

Methylammonium bromocuprate $(MeNH_3)_2CuBr_3$ as a new self-absorption-free solution-processable X-ray scintillator

Sergey A. Fateev,[a,†] Daria E. Belikova,[a,†] Daniil A. Novichkov,[b] Vladimir G. Petrov,[b] Valentina V. Utochnikova,[b] Eugene A. Goodilin[a,b,c] and Alexey B. Tarasov*[a,b]

[a] *Department of Materials Science, M. V. Lomonosov Moscow State University, 119991 Moscow, Russian Federation. E-mail: alexey.bor.tarasov@yandex.ru*

[b] *Department of Chemistry, M. V. Lomonosov Moscow State University, 119991 Moscow, Russian Federation*

[c] *Institute of General and Inorganic Chemistry, Russian Academy of Sciences, 119991 Moscow, Russian Federation*

DOI: 10.1016/j.mencom.2022.07.021

We report the radioluminescent properties of the recently discovered hybrid bromocuprate $(MeNH_3)_2CuBr_3$ in a poly(methyl methacrylate) matrix in the form of solution-produced composite thick films. The obtained films demonstrate bright turquoise photoluminescence in UV light and intense radioluminescence due to CuKα and AgKα radiation at room temperature, exceeding the radioluminescence intensity of Cs_4PbBr_6@$CsPbBr_3$ films by more than an order of magnitude.

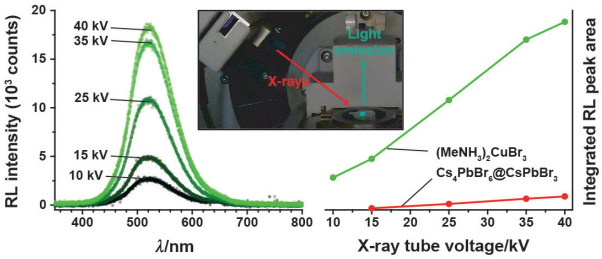

Keywords: hybrid copper halides, bromocuprate, scintillator, radioluminescence, photoluminescence, X-ray imaging.

Scintillation detectors are indispensable components of state-of-the-art devices used for X-ray imaging in computed tomography, radiography, security inspection systems, as well as for the detection of ionizing radiation.[1,2] However, most commercial scintillation materials[3] such as CsI:Tl and $LaBr_3$:Ce are extremely hygroscopic or expensive due to the use of energy-consuming single crystal growth techniques (*e.g.*, the widely used Czochralski method), rare elements or both.[4] Recently, in connection with the growing interest in lead halide perovskites, a new concept of polycrystalline scintillation screens has emerged, which implies the fabrication of a composite based on emitting scintillator nanocrystals in a transparent matrix.[5,6] The implementation of this concept facilitates the deposition of large area flexible scintillation screens using simple and cheap techniques such as blade coating. Despite impressive progress in achieving low X-ray detection limits (down to 13 nGy s^{-1}),[5] the application of scintillators based on lead halide perovskites is hindered by the high toxicity of lead, as well as rather low light yields (LYs).

The newest research suggests that copper halide-based semiconductors can overcome both of these disadvantages of lead halide perovskites. Over the past two years, numerous studies have demonstrated superior luminescence quantum yields for these compounds in the form of single crystals, nanocrystals and powders.[7,8] Having a large Stokes shift of luminescence, low-dimensional halocuprates are characterized by a negligible level of self-absorption.[9,10] Therefore, they can be successfully used in the form of thick millimeter-scale coatings necessary for efficient absorption of X-rays. As a result, high and even record-breaking LYs have been found for many halocuprates, including Rb_2CuBr_3 single crystals (LY 91056 photons MeV^{-1}),[9] $Cs_3Cu_2I_5$ nanocrystals (LY 79279 photons MeV^{-1})[11] and K_2CuBr_3 single crystals (LY 23806 photons MeV^{-1}).[12]

Surprisingly, according to Lian *et al.*,[13] even low-density hybrid halocuprate compounds with large tetrabutylammonium (TBA) cations demonstrate LY at the same level as the well-known dense inorganic scintillator LYSO: for example, the reported LY of $(TBA)CuBr_2$ is 24134 photons MeV^{-1}. At the same time, the scintillation properties of hybrid halocuprates with small size cations are still poorly explored. As far as we know, the sole example is $(MeNH_3)Cu_2I_3$, which exhibits photoluminescence (PL) and radioluminescence (RL) only at low temperatures.[14,15] Herein we describe the scintillation and optical properties of the recently discovered[16] methylammonium bromocuprate $(MeNH_3)_2CuBr_3$ and propose a facile technique for its preparation as robust composites in a polymer matrix.

The $(MeNH_3)_2CuBr_3$ powder was obtained by the reaction of two finely ground powders of CuBr and $(MeNH_3)Br$ precursors in an isopropanol solution upon prolonged stirring.[‡] According to XRD data[§] [Figure 1(*a*)], the resulting white

† These authors contributed equally.

‡ CuBr (143.5 mg) and $(MeNH_3)Br$ (224 mg) were added to a saturated solution of $(MeNH_3)Br$ in isopropanol (2 ml) followed by addition of HBr (24 μl) and H_3PO_2 (5 μl) and stirred for 10 h.

§ Powder X-ray diffraction (XRD) patterns were recorded on a Bruker Advance D8 diffractometer with CuKα radiation in the Bragg–Brentano geometry for 2θ in the range of 5–50° with a step of 0.02°.

PL and PL excitation (PLE) spectra were measured on a FluoroMax Plus spectrophotometer with xenon lamp excitation using an integrating sphere. The PL spectrum at 77 K was recorded on an Ocean Optics FLAME-T-VIS-NIR-ES CCD spectrometer using a UV lamp (λ = 254 nm) as an excitation source.

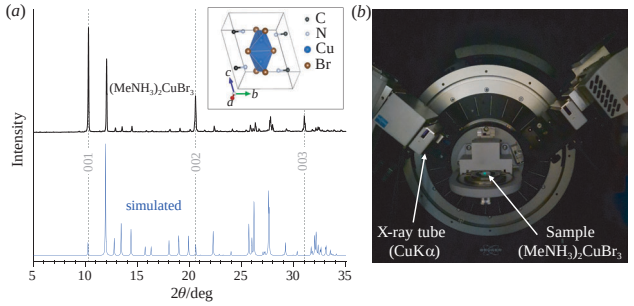

Figure 1 (*a*) Powder XRD pattern of $(MeNH_3)_2CuBr_3$. Inset: crystal structure of the $(MeNH_3)_4Cu_2Br_6$ phase. (*b*) Photograph of the powdered $(MeNH_3)_2CuBr_3$ sample emitting RL induced by CuKα radiation.

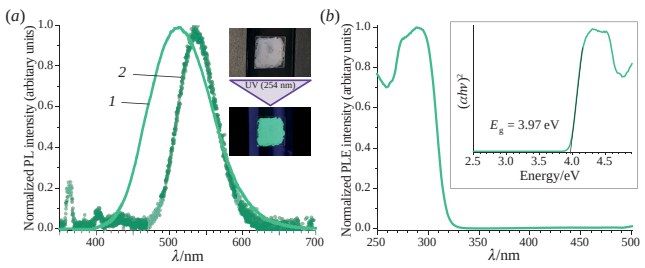

Figure 2 (*a*) PL spectra of the MA213 film measured (*1*) in an integrating sphere at room temperature and (*2*) under UV lamp at 77 K (peaks near 365 and 405 nm are emission lines of the mercury UV lamp). Inset: photographs of the MA213 composite film in daylight and under UV illumination. (*b*) PLE spectrum of the MA213 film recorded at an emission wavelength of 513 nm and the corresponding Tauc plot in the inset.

powder contains a single triclinic (space group $P\bar{1}$) phase of the recently discovered[16] methylammonium bromocuprate $(MeNH_3)_4Cu_2Br_6$ [Figure 1(*a*), inset] and has a noticeable texturing in the [001] direction. It is interesting that even when irradiated with an X-ray tube with a Cu anode ($\lambda_{CuK\alpha1}$ = 1.540562 Å and $\lambda_{CuK\alpha2}$ = 1.544398 Å), the $(MeNH_3)_2CuBr_3$ powder exhibits green RL visible to the naked eye [Figure 1(*b*)]. This same bright turquoise PL is exhibited by the $(MeNH_3)_2CuBr_3$ powder when illuminated with a UV lamp (λ = 254 nm).

For the convenience of measurements, the finely ground powder was dispersed in a solution of poly(methyl methacrylate) (PMMA) in toluene and cast onto the surface of quartz glasses.¶ The obtained composite films of $(MeNH_3)_2CuBr_3$ in the PMMA polymer matrix (hereinafter MA213) are characterized by mechanical durability and a good protection of the material from degradation under the action of moisture. The PL spectrum of the MA213 film at room temperature exhibits the peak centered at 513 nm (2.42 eV) with a full width at half maximum (FWHM) of about 104 nm (42 meV) [Figure 2(*a*)], which is in good agreement with the spectroscopic data of the corresponding single crystals.[16] Upon cooling to liquid nitrogen temperature (~77 K), the MA213 film exhibits a slight redshift of the PL maximum (~536 nm) with a simultaneous significant narrowing of the peak (FWHM ~25 meV). Such a change in PL coincides with that for single crystals and is characteristic of radiative recombination through self-trapped excitons.[13,17]

The PLE spectrum‡ of $(MeNH_3)_2CuBr_3$ has a sharp absorption edge and a well-pronounced excitonic absorption band centered at 290 nm, which indicates a large Stokes shift of 223 nm and additionally confirms the self-trapped mechanism of luminescence. According to the Tauc plot fitting assuming a direct transition, the optical bandgap of $(MeNH_3)_2CuBr_3$ is 3.97 eV [Figure 2(*b*), inset]. Thus, the use of optical methods revealed the absence of self-absorption and impurity absorption or emission in the obtained polycrystalline composite material, which makes it promising for X-ray scintillation.

Like the $(MeNH_3)_2CuBr_3$ powder, the PMMA-based composite film under non-monochromatic radiation from X-ray tubes with both Cu and Ag anodes exhibits RL visible in the dark.‡ As in the PL spectrum, the peak in the RL spectrum is centered at 514 nm, but has a slightly smaller FWHM (~85 nm) [Figure 3(*a*)]. The position and shape of the peak remain unchanged for different X-ray sources and at different voltages for the tube with a silver anode [Figure 3(*c*)]. At the same time, the integral RL intensity increases almost linearly with increasing voltage [Figure 3(*d*)]. The slowdown in the RL intensity growth at high powers may be due to the partial degradation of the material upon exposure to a high dose of radiation.

To quantify the RL of the MA213 film, we compared it with that of a composite consisting of the '0D@3D' halide perovskite Cs_4PbBr_6@$CsPbBr_3$ in a PMMA matrix (hereinafter Cs416), a material characterized by bright PL with a quantum yield of 60%, LY ~6000 photons MeV^{-1} and high reproducibility of synthesis.[6] The PL quantum yield of Cs416 films measured with an integrating sphere was calculated to be about 49%. This is slightly less than originally reported (60%) and indicates a close and relatively low degree of non-radiative recombination. At the same time, it may be expected that, at a much higher linear attenuation coefficient [Figure 3(*b*)] and the same film thickness, Cs416 should absorb a much larger fraction of radiation and, therefore, have a higher light output than $(MeNH_3)_2CuBr_3$. Nevertheless, the MA213 films exhibited an integrated RL intensity 13–25 times higher than that of Cs416, depending on the X-ray tube voltage at which the measurements were made [see Figure 3(*d*)]. It should be noted that, although the $(MeNH_3)_2CuBr_3$ phase does not contain heavy elements, its linear attenuation coefficient is comparable to that of silicon, which is widely used in semiconductor X-ray detectors, and in the region up to 33 keV exceeds the value for the efficient commercial NaI:Tl scintillator.

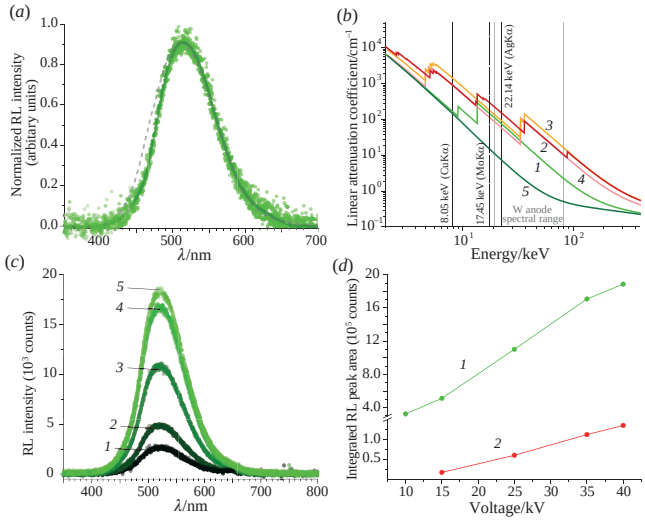

Figure 3 (*a*) Raw (dots) and smoothed (solid line) RL spectra of $(MeNH_3)_2CuBr_3$ compared to the PL spectrum (dashed line). (*b*) Linear attenuation coefficient of (*1*) $(MeNH_3)_2CuBr_3$ compared to conventional X-ray detector materials: (*2*) Cs_4PbBr_6, (*3*) CsI, (*4*) NaI and (*5*) Si. (*c*) MA213 RL spectra measured at different X-ray tube voltages: (*1*) 10, (*2*) 15, (*3*) 25, (*4*) 35 and (*5*) 40 kV. (*d*) Voltage dependence of the integrated RL peak area for (*1*) MA213 and (*2*) Cs416 films.

All RL spectra were obtained using a glass X-ray diffraction tube (XRD Eigenmann GmbH) with a Be window suppressing radiation below 4 keV as an X-ray source. The size of the radiation spot on the samples was about 6 × 6 mm. The spectra were recorded using an Ocean Optics USB4000+ spectrometer equipped with an optical fiber.

¶ $(MeNH_3)_2CuBr_3$ powder (200 mg) was dispersed in a PMMA solution (200 mg ml^{-1}) in toluene and cast onto quartz glass to form a 200 μm thick solid film.

To estimate the LY of the new scintillator, the RL intensity of the obtained MA213 films with a thickness of ~200 μm was compared with that of a commercial ceramic X-ray phosphor made of gadolinium oxysulfide (Gd_2O_2S) with a LY of about 50 000 photons MeV^{-1}.[18] The integrated intensity of the X-ray luminescence peak of the $(MeNH_3)_2CuBr_3$ powder was about 30% of that for Gd_2O_2S:Tb. Since the Gd_2O_2S:Tb material has the same polycrystalline state as $(MeNH_3)_2CuBr_3$ in the polymer matrix, the measurements of the RL intensity of Gd_2O_2S:Tb and MA213 were carried out in the same geometry with irradiation of equal areas with X-rays and registration of luminescence from above the sample. Under such conditions, we assume a direct proportionality between the measured integrated RL intensity for both materials and estimate the LY for $(MeNH_3)_2CuBr_3$ at 13 700 photons MeV^{-1}, which is comparable with the other hybrid[13] and inorganic[12] bromocuprates.

In summary, we propose simple procedures for the synthesis of $(MeNH_3)_2CuBr_3$ powder and the fabrication of robust thick films based on its fine powder in a PMMA matrix. The resulting composite films are characterized by intense PL, a large Stokes shift (~223 nm) and a negligible level of self-absorption. For the first time, the phenomenon of intense RL of the hybrid bromocuprate $(MeNH_3)_2CuBr_3$ at room temperature is observed. The position of the maximum and the shape of the RL spectrum almost coincide with those of the PL spectrum, which indicates a similar mechanism of radiative recombination. The RL intensity of $(MeNH_3)_2CuBr_3$ composite films is more than an order of magnitude higher than that of similarly prepared Cs_4PbBr_6@$CsPbBr_3$ films, which previously proved to be a promising material for X-ray imaging. Finally, the $(MeNH_3)_2CuBr_3$ phase may be of interest for the fabrication of cheap scintillation screens and opens up prospects for studying the scintillation properties of other hybrid halocuprates.

This work was supported by the Russian Foundation for Basic Research (project no. 20-33-70265). The authors are grateful to colleagues from the Joint Research Center for Physical Methods of Research of IGIC RAS for valuable assistance in XRD measurements. D.A.N. acknowledges the financial support of the Ministry of Science and Higher Education of the Russian Federation (grant no. 075-15-2019-1891) for RL measurements.

References

1 M. Nikl and A. Yoshikawa, *Adv. Opt. Mater.*, 2015, **3**, 463.
2 M. J. Yaffe and J. A. Rowlands, *Phys. Med. Biol.*, 1997, **42**, 1.
3 M. Nikl, *Meas. Sci. Technol.*, 2006, **17**, R37.
4 M. J. Weber, *J. Lumin.*, 2002, **100**, 35.
5 Q. Chen, J. Wu, X. Ou, B. Huang, J. Almutlaq, A. A. Zhumekenov, X. Guan, S. Han, L. Liang, Z. Yi, J. Li, X. Xie, Y. Wang, Y. Li, D. Fan, D. B. L. Teh, A. H. All, O. F. Mohammed, O. M. Bakr, T. Wu, M. Bettinelli, H. Yang, W. Huang and X. Liu, *Nature*, 2018, **561**, 88.
6 F. Cao, D. Yu, W. Ma, X. Xu, B. Cai, Y. M. Yang, S. Liu, L. He, Y. Ke, S. Lan, K.-L. Choy and H. Zeng, *ACS Nano*, 2020, **14**, 5183.
7 Y. Li, Z. Zhou, N. Tewari, M. Ng, P. Geng, D. Chen, P. K. Ko, M. Qammar, L. Guo and J. E. Halpert, *Mater. Chem. Front.*, 2021, **5**, 4796.
8 J. Yin, Q. Lei, Y. Han, O. M. Bakr and O. F. Mohammed, *Phys. Status Solidi RRL*, 2021, **15**, 2100138.
9 B. Yang, L. Yin, G. Niu, J.-H. Yuan, K.-H. Xue, Z. Tan, X.-S. Miao, M. Niu, X. Du, H. Song, E. Lifshitz and J. Tang, *Adv. Mater.*, 2019, **31**, 1904711.
10 X. Zhao, G. Niu, J. Zhu, B. Yang, J.-H. Yuan, S. Li, W. Gao, Q. Hu, L. Yin, K.-H. Xue, E. Lifshitz, X. Miao and J. Tang, *J. Phys. Chem. Lett.*, 2020, **11**, 1873.
11 L. Lian, M. Zheng, W. Zhang, L. Yin, X. Du, P. Zhang, X. Zhang, J. Gao, D. Zhang, L. Gao, G. Niu, H. Song, R. Chen, X. Lan, J. Tang and J. Zhang, *Adv. Sci.*, 2020, **7**, 2000195.
12 W. Gao, G. Niu, L. Yin, B. Yang, J.-H. Yuan, D. Zhang, K.-H. Xue, X. Miao, Q. Hu, X. Du and J. Tang, *ACS Appl. Electron. Mater.*, 2020, **2**, 2242.
13 L. Lian, X. Wang, P. Zhang, J. Zhu, X. Zhang, J. Gao, S. Wang, G. Liang, D. Zhang, L. Gao, H. Song, R. Chen, X. Lan, W. Liang, G. Niu, J. Tang and J. Zhang, *J. Phys. Chem. Lett.*, 2021, **12**, 6919.
14 A. A. Petrov, V. N. Khrustalev, Y. V. Zubavichus, P. V. Dorovatovskii, E. A. Goodilin and A. B. Tarasov, *Mendeleev Commun.*, 2018, **28**, 245.
15 A. A. Petrov, S. A. Fateev, A. Yu. Grishko, A. A. Ordinartsev, A. V. Petrov, A. Yu. Seregin, P. V. Dorovatovskii, E. A. Goodilin and A. B. Tarasov, *Mendeleev Commun.*, 2021, **31**, 14.
16 H. Peng, S. Yao, Y. Guo, R. Zhi, X. Wang, F. Ge, Y. Tian, J. Wang and B. Zou, *J. Phys. Chem. Lett.*, 2020, **11**, 4703.
17 R. Lin, Q. Zhu, Q. Guo, Y. Zhu, W. Zheng and F. Huang, *J. Phys. Chem. C*, 2020, **124**, 20469.
18 P. Lecoq, *Nucl. Instrum. Methods Phys. Res., Sect. A*, 2016, **809**, 130.

Received: 1st December 2021; Com. 21/6768